small NANO MICRO

Self-Assembly

I-Motif Nanospheres: Unusual Self-Assembly of Long Cytosine Strands

Dragoslav Zikich, Ke Liu, Lior Sagiv, Danny Porath, and Alexander Kotlyar**

The synthesis and characterization of novel DNA structures based on tetraplex cytosine (C) arrangements, known as i-motifs or i-tetraplexes, is reported. Atomic force microscopy (AFM) investigation shows that long C-strands in mild acidic conditions form compact spherically shaped nanostructures. The DNA nanospheres are characterized by a typical uniform shape and narrow height distribution. Electrostatic force microscopy (EFM) measurements performed on the i-motif spheres clearly show their electrical polarizability. Further investigations by scanning tunneling microscopy (STM) at ultrahigh vacuum reveals that the structures exhibit an average voltage gap of 1.9 eV, which is narrower than the voltage gap previously measured for poly(dG)–poly(dC) molecules in similar conditions.

1. Introduction

Noncanonical pairing of nuclear bases can create a variety of DNA secondary structures. One of the most interesting DNA forms, arising from the arrangement of cytosine (C)-rich oligonucleotides at low pH is the C-teteraplex or i-motif.[1] Nuclear magnetic resonance (NMR) and X-ray diffraction studies of protonated short C-rich oligonucleotides have revealed an unusual structure composed of two parallel-stranded cytosine duplexes, intercalated with each other in an antiparallel orientation.[1–3] Such a duplex structure is held by two cytosines protonated at the N3 position, promoting a C–C^+ base pairing. The geometry of the i-motif structure substantially differs from either double-stranded or guanine-made G-quadruplex DNA forms.[4,5]

In vitro studies have shown that cytosine-rich genomic DNA sequences at mild acidic or even neutral pH can associate both inter- and intra-molecularly to form i-motifs.[6–10] The C-rich sequences naturally occur at numerous sites in the prokaryote genome, where they are supposed to play an important role in gene-regulation processes,[11–14] possibly by formation of i-motif secondary structures. These structures have also attracted substantial interest in nanotechnology.[15] The pH-induced reversible transformation of the i-motif into an unstructured C-strand was utilized for the development of various applications, such as proton-driving chemical oscillators,[16] cellular pH indicators,[17] nanomotor units,[18] or nanoparticle assemblies.[19] In addition, i-motifs can serve as a building material for structural DNA nanotechnology. Recent study has shown that incompletely intercalated i-motif tetraplex building blocks are capable of integrating into hundreds-of-nanometer-long linear nanowires.[20]

The specific geometry of the i-motif causes a closer stacking of bases than in regular DNA. The distance between adjacent cytosines in the i-motif (3.1 Å) is shorter than the distance between base pairs in a Watson–Crick double helix (3.4 Å). It was speculated that a linear arrangement of protons in the core of the structure and shorter distance between

D. Zikich, Prof. A. Kotlyar
Department of Biochemistry George S. Wise Faculty of Life Sciences
Tel Aviv University Ramat Aviv 69978, Israel
E-mail: s2shak@post.tau.ac.il
Dr. K. Liu, L. Sagiv, Prof. D. Porath
Institute of Chemistry
The Hebrew University
Jerusalem 91904, Israel
E-mail: porath@chem.ch.huji.ac.il
Prof. D. Porath
Center for Nanoscience and Nanotechnology
The Hebrew University
Jerusalem 91904, Israel
Prof. A. Kotlyar
The Center for Nanoscience and Nanotechnology
Tel Aviv University
Ramat Aviv, 69978, Israel

DOI: 10.1002/smll.201002213

the bases may lead to improved electrical properties with respect to canonical DNA.[20]

We have previously reported the formation of long G-quadruplex nanowires from long homopolymeric guanine strands.[21] In this paper, we study folding of long DNA strands composed of hundreds of C bases into tetraplex structures. The molecular morphology and properties of the structures are characterized by atomic force microscopy (AFM), electrostatic force microscopy (EFM), and scanning tunneling microscopy (STM). We show the formation of compact nanometric spherical structures that exhibit remarkably uniform shape and clear electrical polarizability.

2. Results

Long poly(dC) molecules of specific and uniform length were achieved through a combination of synthesis and separation techniques, as described earlier.[22,23] As a starting material for preparation of i-motif structures, we used homogeneous solutions of C-strands, obtained using size-exclusion high-performance liquid chromatography (HPLC). The pH of the solution containing C-strands was decreased during the dialysis against 20 nM tris-acetate (pH 4.5), from 13.0 to 4.5. Spectroscopic analysis of the DNA sample before (pH 13) and after (pH 4.5) the dialysis is shown in **Figure 1**. As can be seen from Figure 1B (red trace), reduction of pH caused a decrease in the absorption maxima and a redshift, which are clear indications for DNA-strand folding. The structural transition of the C-strands upon pH decrease was examined by circular dichroism (CD) spectroscopy. It was demonstrated for short C-rich oligonucleotide sequences that the CD spectrum of an i-motif exhibits a positive band around 285 nm and a negative band around 265 nm.[6,10] The CD spectrum of a long C-strand solution at mild acidic pH, presented in Figure 1C (red trace), shows a typical i-motif CD signature (positive signal at 288 nm and a negative one at 265 nm), in contrast to alkali solution of the strands (Figure 1C, blue trace).

The morphology of the long strands was further investigated by AFM. The AFM images showed that the strands being deposited on mica from mild acidic solution adopt unusual spherical shapes (**Figure 2**A). The spherical structures display remarkably uniform size and shape, as shown in the insets of Figure 2A. In contrast, AFM analysis of a sample of C-strands deposited from 20 mM tris-acetate (pH 8) lack spherical structures (data not presented). Statistical AFM morphology analyses conducted on >100 single spherical structures from different mica areas showed an average height of ≈7.0 ± 0.8 nm (see Figure 2B). We further examined the consistency of spherical arrangement by performing the comparative experiments with poly(dC) molecules of different lengths (0.8, 1.2, and 2.0 Kb). The CD spectroscopy and AFM imaging showed that all the above poly(dC) strands fold into i-motif nanospheres at mild acidic pH. The average heights of nanospheres on a mica surface are 5.1 ± 0.7, 6.2 ± 0.8, and 8.1 ± 1.0 nm for the structures originating from 0.8-, 1.2-, and 2.0-Kb-long poly(dC), respectively (see Figure 2C). As seen in the figure, the size (height) of the sphere linearly depends on the amount of C-bases in the strand. It is important to note that various double-stranded DNA types, like random sequence pUC19, GC (guanine–cytosine) and AT (adenine–thymine) homopolymers, as well as long G4 wires deposited on a mica surface under identical conditions, adopt a linear conformation.

The stability of the i-motif is governed by the protonation state of cytosine bases in the strand. Since the pK_a of cytosine is 4.2, the maximum stabilization of the structure is achieved under mild acidic conditions (pH 4–4.5), where the concentration of both the protonated and the deprotonated forms of the base is nearly equal. Deprotonation of the base, caused by the pH increase, leads to destabilization of the structure.[8,9,24] We have investigated the stability of i-motifs made of C-strands of various lengths, namely: $(dC)_{20}$, $(dC)_{800}$, $(dC)_{1200}$, and $(dC)_{2000}$, at different pH. The i-motif structures, prepared as described above, were further exposed for 10 min to media of different pH. The pH-induced reversible transition of the C-strand from tetraplex to an unfolded single-stranded form was followed by CD spectroscopy through the monitoring of a positive peak at 288 nm, characteristic of the i-motif.[10] **Figure 3** shows the pH dependence of the intensity of the CD signal at 288 nm for C-strands of different lengths. It is clearly seen from the figure that i-motif structures composed

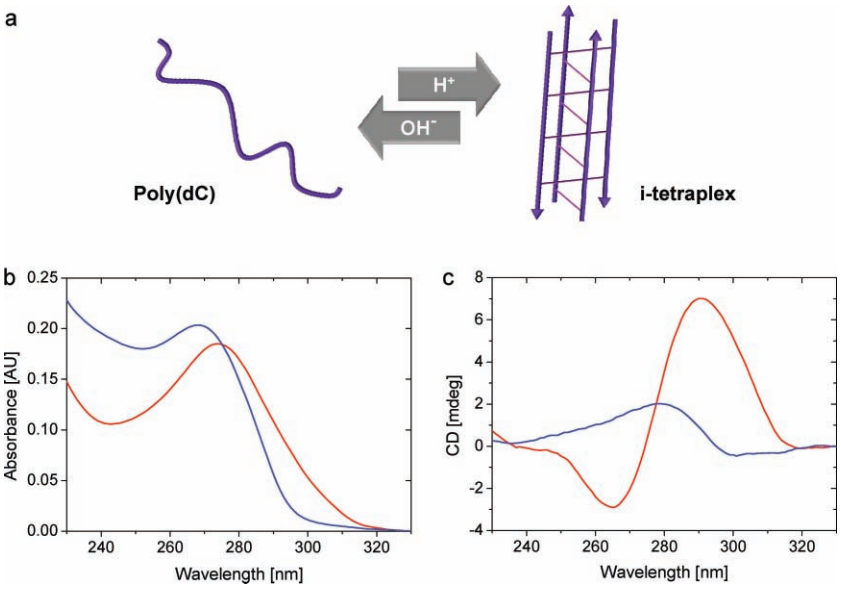

Figure 1. a) Schematic presentation of a long poly(dC) strand at high and low pH. At high pH, the molecule lacks secondary structure, while at mild acidic pH, the strand undergoes spontaneous reversible transformation into the i-motif, composed of two intercalated parallel-stranded duplexes. b) UV absorption and c) CD spectra of 1.5-Kb-long C-strands in 0.1 M NaOH (blue traces) and in 20 mM tris-acetate (pH 4.5) (red traces).

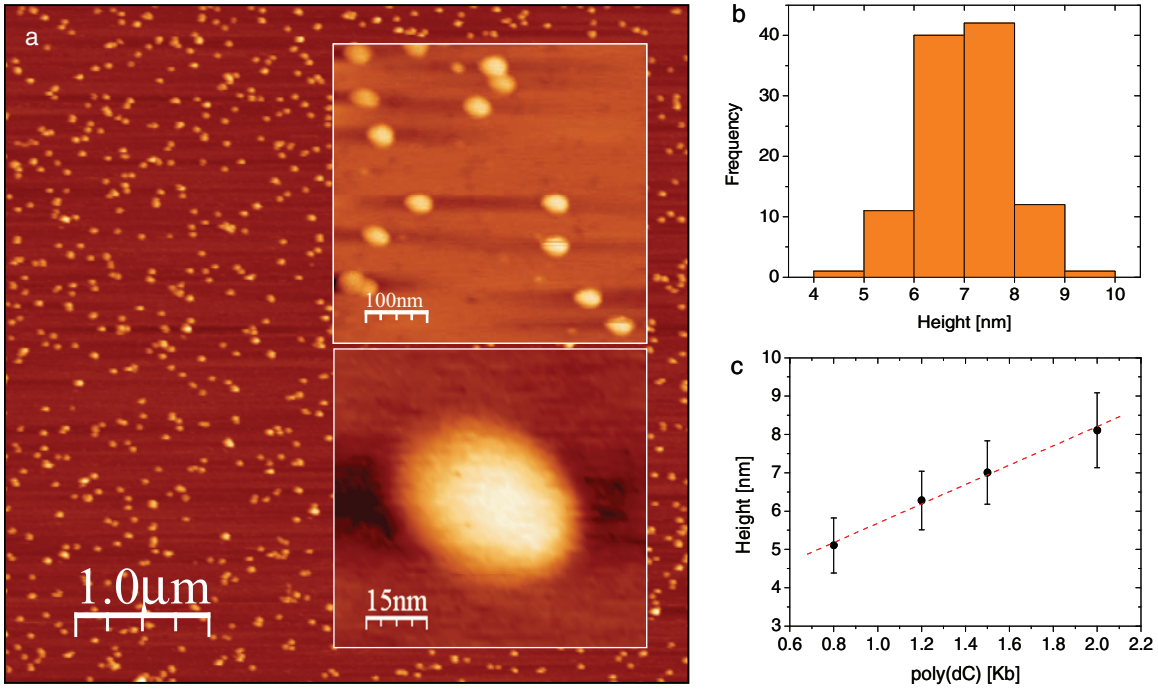

Figure 2. AFM analysis of i-motif structures. a) AFM image of 1.5 Kb poly(dC); 20 μL of 0.2 nM DNA samples (in molecules) in 20 mM tris-acetate (pH 4.5), containing 2 mM $MgCl_2$, were incubated on mica plates for 2–5 min. The insets show higher resolution images of the structures. b) Height-distribution histogram of >100 single well separated spherical bodies. c) Correlation between the apparent height of the spherical structures and the number of bases in the C-strand.

of long C-strands (800 bases or more) are stable at pH 7, while short $(dC)_{20}$ strands lose the i-motif characteristics at pH above 6. The pH-dependent structural behavior of $(dC)_{20}$ is consistent with earlier results obtained using short cytosine oligonucleotides.[9,10,24]

As shown in our previous works, EFM is a useful tool to examine the polarizability of molecular materials.[25–27] The polarizability is identified by the phase shift between the voltage-induced and the actual tip oscillations, appearing as dark areas in the phase image. We performed EFM measurements on single spherical i-motif structures composed of 800-base-long C-strands. An example of the EFM measurements is shown in **Figure 4**A. Phase shifts were registered when applying different biases at 20-nm lift above the imaging set point. The negative phase shift was detected at both +4 and −4 V, indicating that the electrostatic interaction is due to the polarizability of the structure and not due to charging of the object. The phase shift of the spherical structures, measured at the above conditions, was −0.30 and −0.34 mV at +4 and −4 V, respectively. A similar polarizability effect was observed in measurements done on different samples, tips, and AFM systems. It is worth noting that a 800-bp double-stranded poly(dG)–poly(dC) molecule, containing the same amount of cytosine bases as the spherical structures tested here, did not show any phase shift, that is, no polarizability.[26]

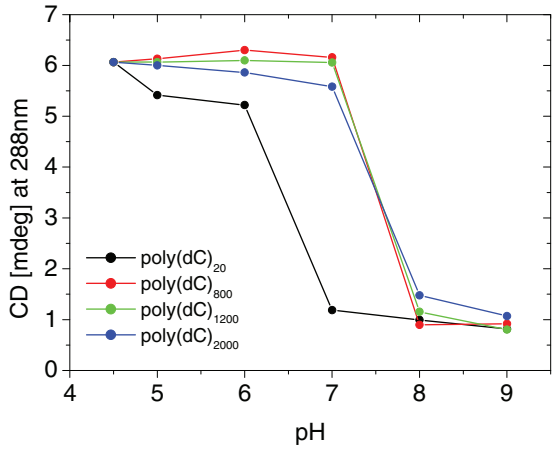

Figure 3. pH dependence of i-motif stability. The CD signal at 288 nm, indicative of i-motif secondary structure, was measured at different pH values for 20- (black), 800- (red), 1200- (green), and 2000- (blue) base-long C-strands.

The electrical properties of the spheres were further investigated by STM. The molecules were measured with an Omicron low-temperature (LT) STM system at room temperature in ultrahigh-vacuum conditions at 5×10^{-11} mbar. A tunneling-junction impedance on the order of giga-ohms enables the avoidance of damage to the target molecules. The STM topography, as shown in **Figure 5**A, is consistent with the AFM topography, showing a pear-like shape with an apparent height of ≈5 nm and width of ≈25 nm. Scanning tunneling spectroscopy (STS) was then used to measure individual molecules with a set-point current of 0.5 nA and bias voltage of 2.5 V. The sample preparation and measurement methods were done as described in detail in our previous reports.[28–31] The corresponding

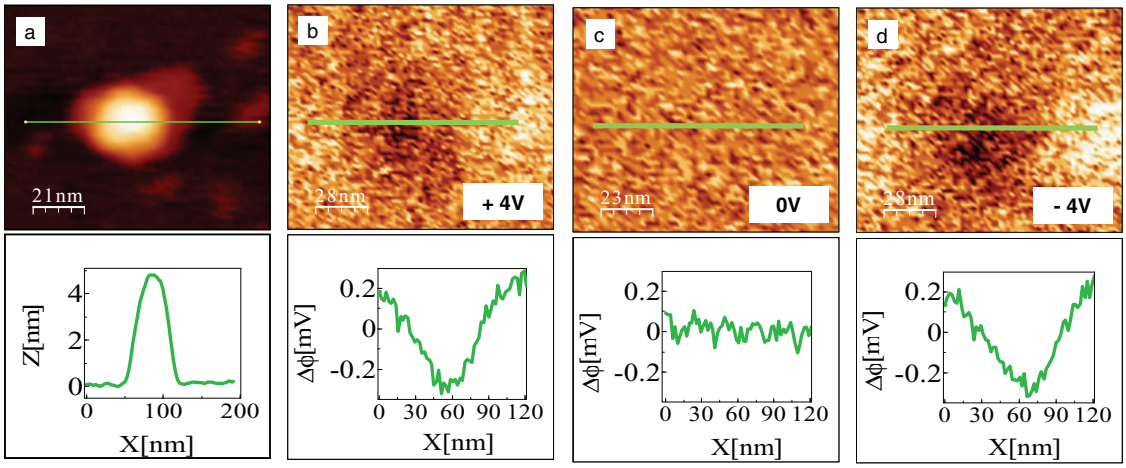

Figure 4. EFM measurements on i-motif spherical structures composed of 800 C-bases. a) A typical topography image and height profile of the molecule. b–d) Phase-shift images and profiles, taken at ≈20 nm, calibrated from force–distance curves, above the imaging set-point with +4, 0, and −4 V, respectively. The dark appearance of molecules in (b) and (d) indicates attraction between the molecules and the biased tip, for both positive and negative voltages and, therefore, polarizability.

differential conductance curves (d*I*/d*V*–*V*) (Figure 5C) of *I*–*V* curves (Figure 5B) displayed an average voltage gap of 1.9 eV, according to the histogram in Figure 5D. Several peaks were found in the voltage-gap distribution, which may be related to various conformations within the molecule structure. Although we did not observe reproducible peaks in conductance curves at this temperature, the voltage gap seems smaller than that of poly(dG)–poly(dC) molecules.[29]

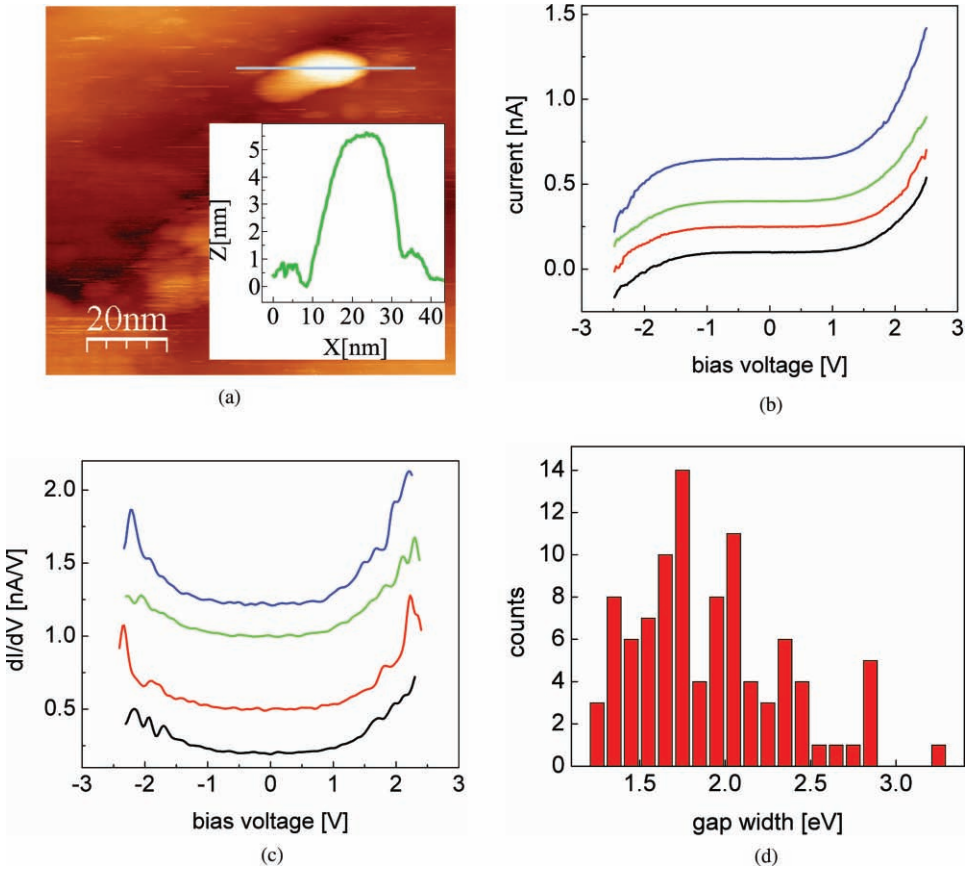

Figure 5. STM and STS measurements on the i-motif nanospheres. Structures composed of 800 C-bases were imaged and measured at room temperature under ultrahigh-vacuum conditions (5×10^{-11} mbar). a) A typical STM image and height profile of the molecule, at a current set point of 20 pA and bias voltage of 2.5 V. b) STS *I*–*V* curves taken on single spherical structures. Each *I*–*V* curve is an average of 3–15 individual curves. The spectra were offset between the neighboring curves for clarity. c) The corresponding derivatives of the *I*–*V* curves presented in (b). The spectra were offset between the neighboring curves for clarity. d) Statistical histogram of the voltage-gap width for the spherical i-motif structure. Several dominant peak populations can be seen, which may be attributed to different conformations within the structure.

NANO MICRO small

3. Discussion

We have shown by CD spectroscopy (see Figure 1C and 3) that long (hundreds of bases) C-strands undergo conformational transition to i-motif structures upon pH reduction from 13 to 4.5. AFM investigation revealed an unusual spherical morphology of the structures. It is known that i-motif structures are rigid and characterized by an extreme helical stretching.[32] The long i-motif structures studied here were therefore expected to adopt a linear rather than a spherical conformation. We can only speculate on the reasons for the spherical arrangement of long C-strands. The strand folding may include the formation of relatively short multiple tetraplex fragments connected to each other by flexible single-stranded links and their subsequent packing into the compact spherical structure. Unfortunately, direct evidence for the structural arrangement of the strand cannot be obtained using NMR spectroscopy due to the large size of the molecules.

The spherical shape and the narrow size distribution of the structures (see Figure 2) point to a particular C-strand folding pattern. Since the concentration of the strands in the experimental assay was relatively low (20–50 nM), it can be suggested that the spherical structures most likely resulted from monomolecular folding of the C-strands and not from association of several strands. However, direct structural elucidation of the spherical molecules is beyond the scope of this work.

I-motifs made of long C-strands exhibit improved pH stability compared to that formed by short (a few tens of bases) C-oligonucleotides. The latter structures lose the i-motif characteristics at pH above 6, while the spherical structures reported here preserve their i-motif conformation even at neutral pH (see Figure 3). This is probably due to the cooperative stabilization of the spherical structures, which are composed of a large number of C-bases.

We have demonstrated by EFM that the spherical structures exhibit higher electrostatic polarizability, which is absent in linear double-stranded DNA. In addition, the structures are characterized by a smaller voltage gap than the poly(dG)–poly(dC).[29] In view of the above properties, the novel spherical structures present a challenging material for further studies and application in the nanotechnology.

4. Experimental Section

Unless otherwise stated, reagents were obtained from Sigma-Aldrich (USA) and were used without further purification. Klenow fragments of DNA polymerase I from *E. coli* lacking the 3′→5′ exonuclease activity (Klenow exo$^-$) were purchased from Fermentas (Lithuania). The oligonucleotides were purchased from Alpha DNA (Montreal, Canada).

DNA Samples: The oligonucleotides used for DNA synthesis were purchased from Alpha DNA (Montreal, Canada). In biotinylated $(dG)_{12}$ oligonucleotide, the biotin residue is linked to the terminal base at the 5′ end [5′-bio $(dG)_{12}$]. The 5′–bio–$(dG)_{12}$ oligonucleotides were purified on an anion-exchange chromatography column (HiTrap QHP, 5 × 1 mL; Amersham-Biosciences, Sweden) by elution in 0.1 M NaOH and 10% acetonitrile with a linear NaCl gradient from 0.5 to 1 M for 1 h at a flow rate of 0.7 mL min^{-1}. The $(dC)_{12}$ oligonucleotides were purified on an ion-exchange PolyWax LP (liquid-phase) column (4.6 mm × 200 mm, 5 μm, 300 Å; Western Analytical Products, USA). The oligonucleotides were eluted from the column in 10% acetonitrile with a linear K-Pi (pH 7.5) gradient from 20 mM to 0.5 M for 1 h with flow rate of 0.7 mL min^{-1}. Peaks were identified by their retention times obtained from the absorbance at 260 nm. Desalting of purified oligonucleotides was done on prepacked Sephadex G-25 DNA-grade columns (Amersham-Biosciences). The template primer for enzymatic synthesis was prepared by incubation of the purified 5′–biotin–$(dG)_{12}$ oligonucleotides with $(dC)_{12}$ in 0.1 M NaOH at a molar ratio of 1:1 for 15 min and further dialysis of the mixture against 20 mM tris-acetate at pH 7.5 for 2 h. All the oligonucleotides were quantified spectrophotometrically using their respective extinction coefficients of 11.7 and 7.5 mM^{-1} cm^{-1} at 260 nm for $(dG)_{12}$ and $(dC)_{12}$, respectively.[33]

DNA Polymerase Assays: The synthesis of poly(dG)–poly(dC) was performed as described previously.[23] Briefly, the standard reaction contained 60 mM KPi (pH 7.4), 5 mM $MgCl_2$, 5 mM dithioreitol (DTT), and 1.5 mM of deoxyguanosine triphosphate (dGTP) and 1.5 mM deoxycytidine triphosphate (dCTP), 0.2 μM Klenow exo$^-$, and 0.2 μM template-primer, 5′–biotin–$(dG)_{12}$–$(dC)_{12}$. The reaction mixture was incubated at 37 °C for 1–2.5 h, depending on the desirable DNA length, and terminated by the addition of ethylenediaminetetraacetic acid (EDTA) to a final concentration of 20 mM. Reaction products were analyzed by size-exclusion HPLC and by an agarose-gel electrophoresis. 5′–biotin–poly(dG)–poly(dC) produced during the enzymatic synthesis (see above) was separated from single nucleotides and other reaction components by size-exclusion HPLC, using a TSK-gel G-DNA PolyWax column (7.8 mm × 300 mm) (TosoHaas, Japan). The elution was done with 20 mM tris-acetate (pH 8.5) for 30 min at a flow rate of 0.5 mL min^{-1}. The separation was conducted with an Agilent 1100 HPLC system with a photodiode-array detector. Peaks were identified by their retention times obtained from the absorbance at 260 nm.

Preparation of Poly(dC) Strands: Poly(dC) strands of defined lengths were isolated from tetrameric complex between avidin and 5′–bio–poly(dG)–poly(dC) molecules, synthesized and purified as described earlier.[22] The pure complex of avidin attached to four poly(dG)–poly(dC) molecules was pretreated for 20 min at room temperature in 0.1 M NaOH in order to dissociate poly(dG) strands connected to avidin from poly(dC) strands. The separation was carried out with a size-exclusion TSK-gel G-DNA PW HPLC column (7.8 mm × 300 mm; TosoHaas, Japan) by isocratic elution with 0.1 M NaOH for 30 min at a flow rate of 0.5 mL min^{-1}. Peaks were identified by their retention times obtained from the absorbance at 260 and 300 nm. The poly(dC) fraction was collected and used for production of nanostructures. The C-strand concentration was estimated using an extinction coefficient of 7.5 mM^{-1} cm^{-1} at 260 nm.[33]

Spectroscopic Measurements: CD spectra were recorded with a Chirascan circular dichroism spectrometer (Applied Photonics, UK) at 25 °C from 220 to 340 nm with a 1-nm increment and an averaging time of 3 s. Each spectrum was an average of 3 scans. Absorption spectra of DNA samples were recorded with Jasco V-630 spectrophotometer (Japan).

AFM Imaging: AFM was performed on molecules adsorbed onto muscovite mica surfaces. 20 μL of 0.2 nM (in molecules) DNA samples in 2 mM tris-acetate (pH 7.4), containing 2 mM $MgCl_2$,

were incubated on 1-cm × 1-cm freshly cleaved mica plates for 2–5 min, washed with distilled water, and dried with nitrogen gas. AFM images were acquired with two systems: i) A Solver PRO AFM system (NT-MDT, Russia) in semicontact (tapping) mode using 130-μm-long Si–gold-coated cantilevers (NT-MDT, Russia) with a resonance frequency of 119–180 KHz; ii) Images were measured with a Dulcinea AFM system (Nanotec Electronica S.L., Madrid) in dynamic mode. Soft cantilevers (OMCL-RC800PSA, Olympus Optical Co., Ltd.) of nominal force constant 0.3 N m^{-1}, resonance frequency 75–80 kHz, and with a tip radius of 15–20 nm were used (the tip radius was measured with a scanning electron microscope). The cantilever was oscillated at its resonance frequency while the amplitude and the phase, relative to the oscillatory driving force, were measured through the tip-deflection signal as detected by the photodetector. The feedback was performed on the amplitude signal channel. The AFM scanning was processed by the AFM's image-software package. The images were analyzed using WSxM 3.0 imaging software (Nanotec Electronica S.L, Madrid).[34]

EFM Measurements: The electrostatic polarizability of the molecules was checked by EFM using methods described previously.[23–25] The measurements were conducted in retrace mode with a tip lift of ≈20 nm, as calibrated from force–distance curves above the topography set-point height, at 0, −4, and +4 V applied to the tip. The phase-shift signal that is compared for the different molecules at the various voltages is integrated from the cross-sections along the molecule. Conductive tips used in this work were Multi75B soft-tapping mode AFM tips (Budget Sensor, Sofia, Bulgaria) with a nominal spring constant of 3 N m^{-1}, a resonance frequency of 60 KHz, and a tip-apex radius of less than 25 nm.

STM and STS Measurements: The molecules were imaged and measured with a low-temperature Omicron LT-STM system at room temperature in ultrahigh-vacuum conditions at 5×10^{-11} mbar. The tip set-point parameters were 20 pA and 1.5–2.5 V. The sample preparation for the STS and the measurement methods were done as described in details in our previous reports.[28–31] The STS measurements on the individual molecules were performed with a set-point current of 0.5 nA and bias voltage of 2.5 V using grid mode. Topography imaging was performed before and after STS measurements to confirm that no sample drifts or tip penetration into molecules took place.

Acknowledgements

We thank Igor Brodsky for fruitful discussions and technical assistance. This work was supported by European Commission FP6 Information Society Technologies program, grant "DNA-Based Nanodevices", EU FP7 "Nano DNA Sequencing", and by the ISF Converging Technologies program, grant 1714/0. K.L. thanks the Valazzi-Pikovsky postdoctoral scholarship of Hebrew University.

[1] K. Gehring, J.-L. Leroy, M. Gueron, *Nature* **1993**, *363*, 561.
[2] L. Chen, L. Cai, X. Zhang, A. Rich, *Biochemistry* **1994**, *33*, 13540.
[3] C. H. Kang, I. Berger, C. Lockshin, R. Ratliff, R. Moyzis, A. Rich, *Proc. Natl. Acad Sci. USA* **1994**, *91*, 11636.
[4] G. Laughlan, A. I. Murchie, D. G. Norman, M. H. Moore, P. C. Moody, D. M. Lilley, B. Luisi, *Science* **1994**, *265*, 520.
[5] J. T. Davis, *Angew. Chem. Int. Ed.* **2004**, *43*, 668.
[6] N. Khan, A. Avino, R. Tauler, C. Gonzalez, R. Eritja, R. Gargallo, *Biochimie* **2007**, *89*, 1562.
[7] S. Nonin-Lecomte, J. L. Leroy, *J. Mol. Biol.* **2001**, *309*, 491.
[8] A. T. Phan, M. Gueron, J.-L. Leroy, *J. Mol. Biol.* **2000**, *299*, 123.
[9] T. Simonsson, M. Pribylova, M. Vorlickova, *Biochem. Biophys. Res. Commun.* **2000**, *278*, 158.
[10] G. Manzini, N. Yathindra, L. E. Xodo, *Nucleic Acids Res.* **1994**, *22*, 4634.
[11] S. Ahmed, A. Kintanar, E. Henderson, *Nat. Struct. Mol. Biol.* **1994**, *1*, 83.
[12] P. Fojtik, M. Vorlickova, *Nucleic Acids Res.* **2001**, *29*, 4684.
[13] P. Kumar, A. Verma, S. Maiti, R. Gargallo, S. Chowdhury, *Biochemistry* **2005**, *44*, 16426.
[14] V. Mathur, A. Verma, S. Maiti, S. Chowdhury, *Biochem. Biophy. Res. Commun.* **2004**, *320*, 1220.
[15] H. Liu, D. Liu, *ChemInform* **2009**, *40*, 2625.
[16] T. Liedl, F. C. Simmel, *Nano Lett.* **2005**, *5*, 1894.
[17] S. Modi, M. G. Swetha, D. Goswami, G. D. Gupta, S. Mayor, Y. Krishnan, *Nat. Nanotechnol.* **2009**, *4*, 325.
[18] W. Shu, D. Liu, M. Watari, C. K. Riener, T. Strunz, M. E. Welland, S. Balasubramanian, R. A. McKendry, *J. Am. Chem. Soc.* **2005**, *127*, 17054.
[19] W. Wang, H. Liu, D. Liu, Y. Xu, Yang, D. Zhou, *Langmuir* **2007**, *23*, 11956.
[20] H. B. Ghodke, K. Ramya, V. Kasinath, G. V. P. Kumar, N. Chandrabhas, K. Yamuna, *Angew. Chem. Int. Ed.* **2007**, *46*, 2646.
[21] A. B. Kotlyar, N. Borovok, T. Molotsky, H. Cohen, E. Shapir, D. Porath,*Adv. Mater.* **2005**, *17*, 1901.
[22] N. Borovok, N. Iram, D. Zikich, J. Ghabboun, G. I. Livshits, D. Porath, A. B. Kotlyar, *Nucleic Acids Res.* **2008**, *36*, 5050.
[23] A. B. Kotlyar, N. Borovok, T. Molotsky, L. Fadeev, M. Gozin, *Nucleic Acids Res.* **2005**, *33*, 525.
[24] K. Halder, V. Mathur, D. Chugh, A. Verma, S. Chowdhury, *Biochem. Biophys. Res. Commun.* **2005**, *327*, 49.
[25] C. Gomez-Navarro, F. Moreno-Herrero, P. J. de Pablo, J. Colchero, J. Gomez-Herrero, A. M. Baro, *Proc. Natl. Acad. Sci. USA* **2002**, *99*, 8484.
[26] H. Cohen, T. Sapir, N. Borovok, T. Molotsky, R. Di Felice, A. B. Kotlyar, D. Porath, *Nano Lett.* **2007**, *7*, 981.
[27] I. Medalsy, O. Dgany, M. Sowwan, H. Cohen, A. Yukashevska, S. G. Wolf, A. Wolf, A. Koster, O. Almog, I. Marton, Y. Pouny, A. Altman, O. Shoseyov, D. Porath, *Nano Lett.* **2008**, *8*, 473.
[28] E. Shapir, H. Cohen, N. Borovok, A. B. Kotlyar, D. Porath, *J. Phys. Chem. B* **2006**, *110*, 4430.
[29] E. Shapir, H. Cohen, A. Calzolari, C. Cavazzoni, D. A. Ryndyk, G. Cuniberti, A. Kotlyar, R. Di Felice, D. Porath, *Nat. Mater.* **2008**, *7*, 68.
[30] E. Shapir, L. Sagiv, N. Borovok, T. Molotski, A. B. Kotlyar, D. Porath, *J. Phys. Chem. B* **2008**, *112*, 9267.
[31] E. Shapir, J. Yi, H. Cohen, A. B. Kotlyar, G. Cuniberti, D. Porath, *J. Phys. Chem. B* **2005**, *109*, 14270.
[32] A. Lebrun, R. Lavery, *Nucleic Acids Res.* **1996**, *24*, 2260.
[33] C. R. Cantor, M. M. Warshaw, H. Shapiro, *Biopolymers* **1970**, *9*, 1059.
[34] I. Horcas, R. Fernandez, J. M. Gomez-Rodriguez, J. Colchero, J. Gomez-Herrero, A. M. Baro, *Rev. Sci. Instrum.* **2007**, *78*, 013705.

Received: December 4, 2010
Revised: January 14, 2011
Published online: March 7, 2011

